RESEARCH ARTICLE

Gromochytrium mamkaevae gen. & sp. nov. and two new orders: *Gromochytriales* and *Mesochytriales* (*Chytridiomycetes*)

S.A. Karpov[1,2], A.A. Kobseva[2], M.A. Mamkaeva[2], K.A. Mamkaeva[2], K.V. Mikhailov[3,5],
G.S. Mirzaeva[4], V.V. Aleoshin[3,5,6]

Abstract   During the last decade several new orders were established in the class *Chytridiomycetes* on the basis of zoospore ultrastructure and molecular phylogeny. Here we present the ultrastructure and molecular phylogeny of strain x-51 CALU – a parasite of the alga *Tribonema gayanum*, originally described as *Rhizophydium* sp. based on light microscopy. Detailed investigation revealed that the zoospore ultrastructure of this strain has unique characters not found in any order of *Chytridiomycetes*: posterior ribosomal core unbounded by the endoplasmic reticulum and detached from the nucleus or microbody-lipid complex, and kinetosome composed of microtubular doublets. An isolated phylogenetic position of x-51 is further confirmed by the analysis of 18S and 28S rRNA sequences, and motivates the description of a new genus and species *Gromochytrium mamkaevae*. The sister position of *G. mamkaevae* branch relative to *Mesochytrium* and a cluster of environmental sequences, as well as the ultrastructural differences between *Gromochytrium* and *Mesochytrium* zoospores prompted us to establish two new orders: *Gromochytriales* and *Mesochytriales*.

INTRODUCTION

Molecular phylogeny has dramatically changed chytrid taxonomy. Investigation of gene sequences of nearly any species or strain initiates a revision of neighbour taxa and often permits authors to establish new taxa of higher rank, e.g. family, order and class, divisions normally supported by zoospore ultrastructure. In the past few years we have seen several big changes in chytrid taxonomy: Letcher et al. (2006) described the *Rhizophydium* clade (James et al. 2000, 2006) as the order *Rhizophydiales*; Mozley-Standridge et al. (2009) established the order *Cladochytriales* from the *Cladochytrium* clade (James et al. 2006) and Simmons et al. (2009) described the clade formerly represented in phylogenetic trees (James et al. 2006) by *Chytriomyces angularis* as the order *Lobulomycetales*. "This removal of clades from the polyphyletic *Chytridiales* better reflected the diversity of the *Chytridiomycota* and began the corrective process of classifying the *Chytridiomycetes* (chytrids) into phylogenetic groups according to the best tools available." – wrote Longcore and Simmons in the introduction to the new order *Polychytriales* (Longcore & Simmons 2012: 276). This conclusion highlights the fact that we need molecular data for each traditionally described species of *Chytridiomycetes* to construct a meaningful and comprehensive classification of *Chytridiomycetes*.

Rhizophydium is one of the largest genera of *Chytridiomycetes* known from the middle of the 19th century (Rabenhorst 1868). It accounts for more than 225 species, which were described from freshwater, primarily as parasites of algae, and from soil as saprotrophs (Longcore 1996, Letcher et al. 2004). The data on this genus were significantly expanded in recent investigations (Letcher et al. 2006, 2008) and reviewed in a comprehensive taxonomic summary and revision of the genus (Letcher & Powell 2012).

Nevertheless, the list of species investigated with modern methods is still far from being complete, and new data on the ultrastructure and molecular phylogeny of other strains are always important for understanding the huge morphological and genetic diversity of this genus. Moreover, the transmission electron microscopy (TEM) sometimes reveals peculiarities that can be used as new taxonomic characters, or may show the unimportance of some commonly accepted ultrastructural characters.

Here we present the ultrastructure and molecular phylogeny of an algal parasite, strain x-51 CALU, which was described in a preliminary study as 'Rhizophydium sp.'. We show that zoospore ultrastructure of this strain differs from that of other described species, and includes characters not described in any orders of *Chytridiomycetes*. These morphological data confirm an isolated phylogenetic position of x-51 obtained from the analysis of 18S and 28S rRNA sequences, and serve as the basis for the description of a new species and genus. Sister position of the x-51 branch relative to a cluster of environmental sequences, which includes *Mesochytrium penetrans*, and the ultrastructural differences of x-51 and *Mesochytrium* zoospores prompt us to establish two new orders: *Gromochytriales* and *Mesochytriales*.

MATERIALS AND METHODS

Strain CALU x-51 was isolated from a water sample collected from a ditch by the highway near town Kirovsk, Leningrad

[1] Zoological Institute, Russian Academy of Sciences, St. Petersburg 198904, Russian Federation; corresponding author e-mail: sakarpov4@gmail.com.
[2] Biological Faculty, St. Petersburg State University, St. Petersburg 198904, Russian Federation.
[3] A.N. Belozersky Institute for Physico-Chemical Biology, Lomonosov Moscow State University, Moscow 119991, Russian Federation.
[4] Institute of Gene Pool of Plants and Animals, Uzbek Academy of Sciences, 32 Durmon-yuli str., Tashkent 100125, Republic of Uzbekistan.
[5] A.A. Kharkevich Institute for Information Transmission Problems, Russian Academy of Sciences, Moscow 127994, Russian Federation.
[6] National Research Institute of Physiology, Biochemistry, and Nutrition of Farm Animals, Russian Academy of Agricultural Sciences, Borovsk 249013, Kaluga region, Russian Federation.

Table 1   List of rRNA genes used in phylogenetic analysis.

Taxon	Isolate number	GenBank accession no.			Cumulative length (%)
		18S	5.8S	28S	
Outgroup: aphelids and rozellids					
Amoeboaphelidium protococcarum	CALU X-5	JX507298	JX507298	JX507298	99
Rozella allomycis	UCB 47-054 (AFTOL-ID 297)	AY635838	AY997087	DQ273803	99
Rozella sp.	JEL347 (AFTOL-ID 16)	AY601707	AY997086	DQ273766	98
Blastocladiomycota					
Blastocladiella emersonii		M54937	AY997032	X90411	98
Allomyces arbuscula	AFTOL-ID 300	AY552524	AY997028	AY552525	98
Physoderma maydis	AFTOL-ID 19	AY601708	AY997072	DQ273768	96
Neocallimastigomycota					
Neocallimastix sp.	GE13 (AFTOL-ID 638)	DQ322625	AY997064	DQ273822	97
Orpinomyces sp.	OUS1	AJ864616, AJ864475	AJ864475	AJ864475	98
Cyllamyces aberensis	EO14 (AFTOL-ID 846)	DQ536481	AY997042	DQ273829	100
D3	uncultured	EU910609			36
Monoblepharidomycetes					
Monoblepharella mexicana	BK 78-1 (AFTOL-ID 33)	AF164337	AY997061	DQ273777	98
Gonapodya prolifera	JEL478	JGI v. 1.0	JGI v. 1.0	JGI v. 1.0	100
Oedogoniomyces sp.	CR84 (AFTOL-ID 298)	AY635839	AY997066	DQ273804	99
Hyaloraphidium curvatum	SAG 235-1 (AFTOL-ID 26)	Y17504	AY997055	DQ273771	91
PFE7AU2004	uncultured	DQ244008			36
L73_ML_156	uncultured	FJ354068			22
Elev_18S_563	uncultured	EF024210			36
Gromochytriales, ord. nov.					
Gromochytrium mamkaevae	CALU X-51	KF586842	KF586842	KF586842	99
kor_110904_17	uncultured	FJ157331			33
IIN1-34	uncultured		EU516964	EU516964	15
Mesochytriales, ord. nov.					
Mesochytrium penetrans	CALU X-10	FJ804149		FJ804153	37
WS 10-E02	uncultured	AJ867629			34
WS 10-E14	uncultured	AJ867630			36
WS 10-E15	uncultured	AJ867631			36
Spring_08	uncultured	JX069031			11
Spring_37	uncultured	JX069054			11
Spring_57	uncultured	JX069067			11
Spring_71	uncultured	JX069077			11
T2P1AeB05	uncultured	GQ995415			36
T2P1AeF04	uncultured	GQ995412			36
T3P1AeC03	uncultured	GQ995413			36
T5P2AeC07	uncultured	GQ995414			36
SAPA5_E7	uncultured	FJ483310			15
P60E-9	uncultured	DQ104060			13
P60E-29	uncultured	DQ104068			14
Clones from a lake in China	uncultured	JX426910, JX426918, JX426923, JX426937, JX426998, JX427002, JX427011			7
Clones from Lake Bourget (BI74, B1, B43, B44, B46-138, B49, B52, B56, BI78, BI88, BI100, BI104, BI107, BI121, BI123, BI15, BI72, BI76, B86-161, BI5)	uncultured	EF196711, EF196713, EF196728, EF196729, EF196731, EF196734, EF196735, EF196738, EF196745, EF196749, EF196751, EF196753, EF196755, EF196762, EF196763, EF196765, EF196775, EF196776, EF196786, EF196799			20
PFF5SP2005	uncultured	EU162641			36
PFD6SP2005	uncultured	EU162637 3'-end			30
PFA12SP2005	uncultured	EU162643			36
Pa2007C10	uncultured	JQ689425			35
F08_SE1B	uncultured	FJ592495 3'-end			17
ThJAR2B-48	uncultured	JF972676			33
528-O25	uncultured	EF586095			17
GA069	uncultured	HM486988			28
GF29312	uncultured	JX417945			16
PFG9SP2005	uncultured	EU162650			36
PA2009C3	uncultured	HQ191369	HQ191369		40
PA2009B6	uncultured	HQ191400	HQ191400		40
PA2009D8	uncultured	HQ191406	HQ191406		40
PA2009E7	uncultured	HQ191286	HQ191286		40
Va2007BB6	uncultured	JQ689445			35
FV23_1H5	uncultured	DQ310332			29

Table 1 (cont.)

Taxon	Isolate number	GenBank accession no			Cumulative length (%)
		18S	5.8S	28S	
Order *Lobulomycetales*					
Lobulomyces angularis	JEL45 (AFTOL-ID 630)	AF164253	AY997036	DQ273815	100
Lobulomyces angularis	PL70	EF443138	EU352774	EF443143	53
Gen. sp.	AF011	EF432819	EF432819	EF432819	57
Maunachytrium keaense	AF021	EF432822		EF432822	54
CCW64	uncultured	AY180029			35
RSC-CHU-20	uncultured	AJ506002			32
D2P03D7	uncultured	EF100268			29
AY2009B4	uncultured	HQ219419	HQ219419		40
IIS1-20	uncultured		EU517013	EU517013	14
Family *Synchytriaceae*					
Synchytrium decipiens	AFTOL-ID 634	DQ536475	AY997094	DQ273819	91
Synchytrium macrosporum	DUH0009363 (AFTOL-ID 635)	DQ322623	AY997095	DQ273820	99
Synchytrium endobioticum	P-58 and Sluknov	AJ784274, AY854021			36
Synchytrium endobioticum	AS-1	JF795580	JF795579		16
OTU97-188	uncultured			JQ310927	11
OTU97-621	uncultured			JQ311409	11
Order *Polychytriales*					
Polychytrium aggregatum	JEL109 (AFTOL-ID 24)	AY601711	AY997074	AY546686	100
Lacustromyces hiemalis	JEL31	AH009039		HQ901700	49
Arkaya lepida	JEL93 (AFTOL-ID 629)	AF164278	AY997056	DQ273814	100
Neokarlingia chitinophila	JEL510	HQ901766		HQ901703	52
Karlingiomyces asterocystis	JEL572	HQ901769		HQ901708	52
Order *Cladochytriales*					
Cladochytrium replicatum	JEL180 (AFTOL-ID 27)	AY546683	AY997037	AY546688	98
Endochytrium sp.	JEL325	AY349046		AY349081	33
Allochytridium luteum	JEL324 (AFTOL-ID 631)	AY635844	AY997044	DQ273816	97
Nephrochytrium sp.	JEL125	AH009049		EU828511	41
Diplochytridium lagenarium	JEL72	AH009044	AY349109	AY349083	50
Nowakowskiella sp.	JEL127 (AFTOL-ID 146)	AY635835	AY997065	DQ273798	98
Order *Chytridiales*					
Podochytrium dentatum	JEL30 (AFTOL-ID 1539)	AH009055	DQ53650	DQ273838	95
Chytriomyces sp.	JEL378 (AFTOL-ID 1532)	DQ536483		DQ273832	73
Rhizoclosmatium sp.	JEL347-h (AFTOL-ID 20)	AY601709	AY997076	DQ273769	98
Chytriomyces spinosus	JEL59 (AFTOL-ID 1540)	AH009063		DQ273839	86
Chytridiales sp.	JEL187 (AFTOL-ID 39)	AY635825	AY997035	DQ273783	98
Chytriomyces sp.	WB235A (AFTOL-ID 1536)	DQ536486	DQ536498	DQ536493	98
Chytriomyces hyalinus	AFTOL-ID 1537	DQ536487	DQ536499	DQ273836	98
Chytriomyces sp.	JEL341 (AFTOL-ID 1531)	DQ536482		DQ273831	92
Rhizidium endosporangiatum	JEL221 (AFTOL-ID 1534)	DQ536484	DQ536496	DQ273834	100
«*Rhizophydium*» sp.	JEL354 (AFTOL-ID 41)	AY635827	AY997083	DQ273785	100
Phlyctochytrium planicorne	JEL47 (AFTOL-ID 628)	DQ536473	AY997070	DQ273813	99
Order *Spizellomycetales*					
Spizellomyces punctatus	ATCC 48900 (AFTOL-ID 182)	AY546684	AY997092	AY546692	92
Powellomyces sp.	JEL95 (AFTOL-ID 32)	AF164245	AY997075	DQ273776	98
Triparticalcar arcticum	AFTOL-ID 696	DQ536480	AY997096	DQ273826	100
Gaertneriomyces semiglobiferus	BK91-10	AF164247			
Gaertneriomyces semiglobiferus	AFTOL-ID 34		AY997051	DQ273778	99
Order *Rhizophlyctidales*					
Rhizophlyctis rosea	JEL 318 (AFTOL-ID 43)	AY635829	AY997078	DQ273787.	99
Catenomyces sp.	JEL342 (AFTOL-ID 47)	AY635830	AY997033	DQ273789	99
Blyttiomyces helicus	AFTOL-ID 2006	DQ536491			34
P34.43	uncultured	AY642701			36
Order *Rhizophydiales*					
'*Rhizophlyctis*' *harderi*	JEL171 (AFTOL-ID 31)	AF164272	AY997077	DQ273775	98
Rhizophydium sp.	JEL316 (AFTOL-ID 1535)	DQ536485	DQ536497	DQ273835	99
Rhizophydium sp.	JEL317 (AFTOL-ID 35)	AY635821	AY997081	DQ273779	98
Rhizophydium brooksianum	JEL136 (AFTOL-ID 22)	AY601710	AY997079	DQ273770	99
Boothiomyces macrosporum	PL AUS 21 (AFTOL-ID 689)	DQ322622	AY997084	DQ273823	99
Kappamyces laurelensis	AFTOL-ID 690	DQ536478	DQ536494	DQ273824	99
Rhizophydium sphaerotheca	AFTOL-ID 37	AY635823	AY997082	DQ273781	97
Rhizophydium sp.	JEL151 (AFTOL-ID 30)	AF164270	AY997080	DQ273774	96
Entophlyctis sp.	JEL174 (AFTOL-ID 38)	AY635824	AY997049	DQ273782	93
Entophlyctis sp. DU-DC1	DU-DC1	AF164255			20
Entophlyctis helioformis	JEL326 (AFTOL-ID 40)	AY635826	AY997048	DQ273784	97
Homoloaphlyctis polyrhiza	JEL142	AFSM01005055	AFSM01005055	AFSM01005055	99
Batrachochytrium dendrobatidis	AAHL-97-845	AF051932			
Batrachochytrium dendrobatidis	JEL197 (AFTOL-ID 21)		AY997031	AY546693	96
incertae sedis					
18s1-47	uncultured	EU733554			21
18s3 24	uncultured	EU733608			21
LLSG10_1 PML-2011t	uncultured			JN049552	13
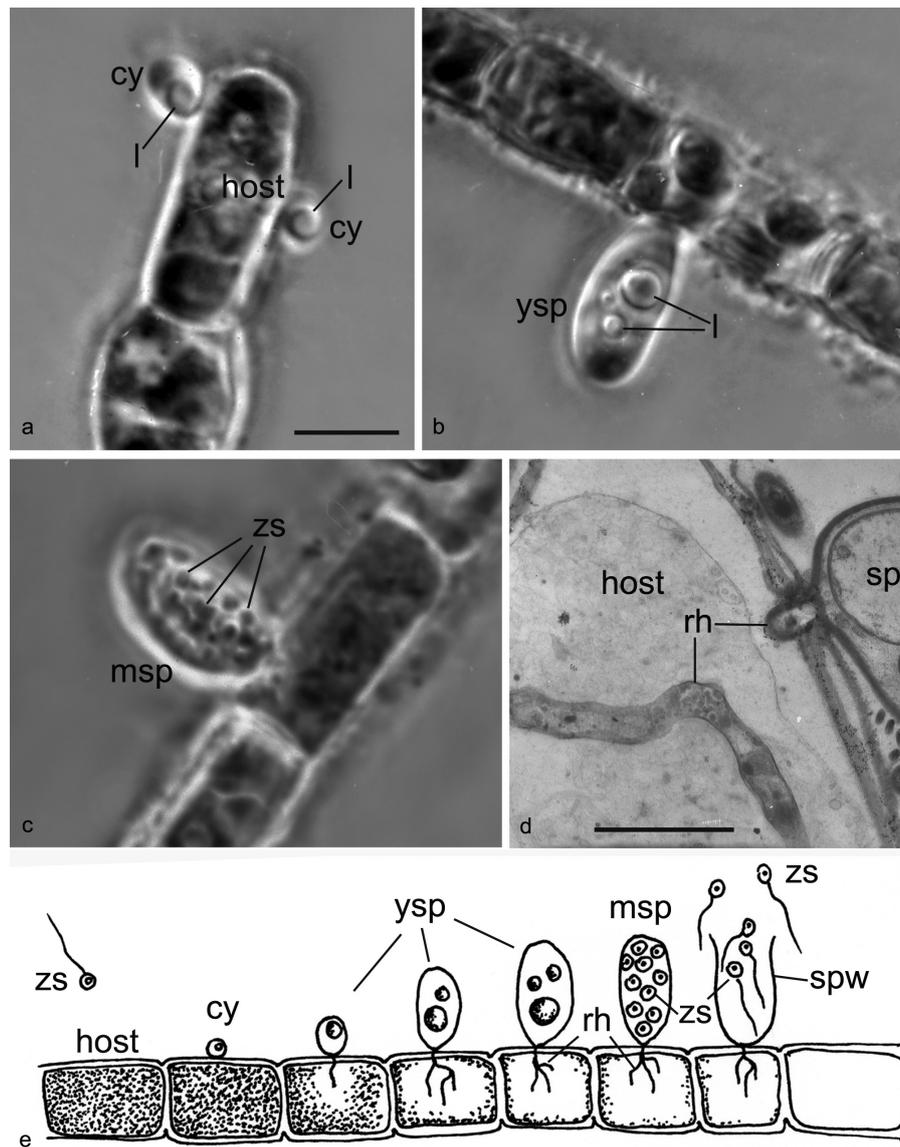
Fig. 1 Stages of the life cycle of *Gromochytrium mamkaevae* (x-51 CALU) on the host *Tribonema gayanum*. — a–c: LM images of living parasite on filament of host *Tribonema*, phase contrast. – a. Two cysts with a lipid globule; b. young sporangium with 3 lipid globules; c. mature sporangium contains zoospores. – d. Rhizoid in the host cell in TEM. – e. Drawing of the life cycle. — Abbreviations: cy = cyst; l = lipid globule; msp = mature sporangium; rh = rhizoid; sp = sporangium; spw = sporangium wall; ysp = young sporangium; zs = zoospores. — Scale bars: a–c = 10 μm; d = 2 μm.

Region (Russia) in the autumn of 1999 by B.V. Gromov, and maintained on the host culture of filamentous, freshwater yellow-green alga *Tribonema gayanum* Pascher CALU 20 cultivated on No. 1 liquid organic medium (Gromov & Titova 1991). A dual clonal culture was incubated at 25 °C under continuous illumination of 25 μmol photon $m^{-2} \cdot s^{-1}$ supplied by 40 W cool white fluorescent tubes.

For light microscopy, the parasite was examined with a Zeiss phase-contrast microscope.
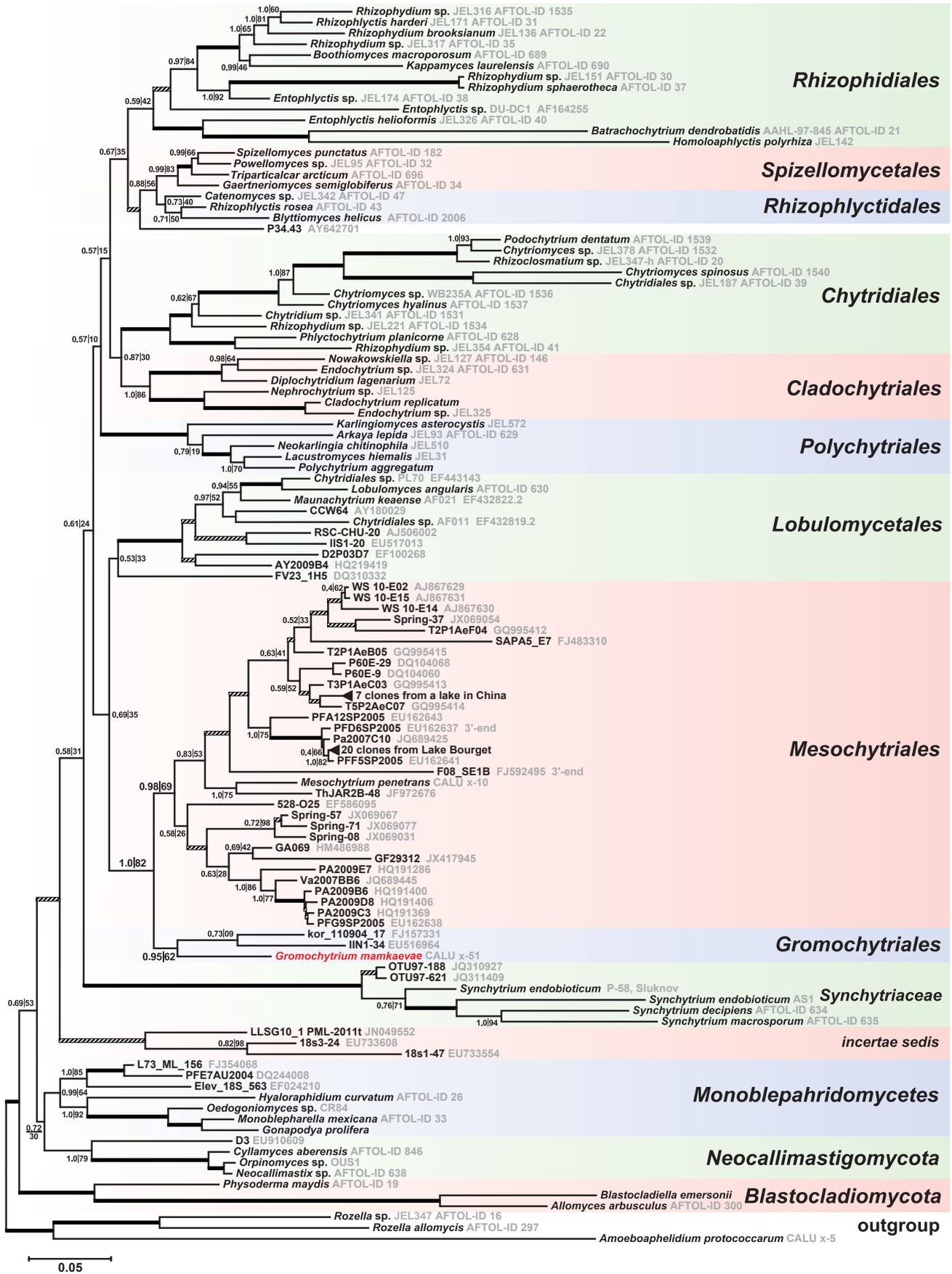
For electron microscopy, the dual culture material was prefixed with 0.5 % OsO_4 for 10 min followed by 2.5 % glutaraldehyde in 0.05 M cacodylate buffer at 4 °C for 2 h. The samples were then incubated with buffered 1 % osmium tetroxide for 1 h at 4 °C. After centrifugation the pellet was dehydrated with a graded ethanol series, and embedded in Spurr's resin. Thin sections were stained with uranyl acetate and lead citrate, and examined with a Jeol 1011 electron microscope at 80 kV.

After inoculation of host strain with x-51, the cultures were incubated until the maximum infection of host cells was reached. Zoospores were then harvested by centrifugation and used directly for DNA extraction. The DNA was extracted with Diatom

DNA Prep (IsoGen Lab, Moscow). The rRNA gene sequences were amplified using Encyclo PCR kit (Evrogen, Moscow) and a set of primers (Medlin et al. 1988, van der Auwera et al. 1994) and sequenced directly with Applied Biosystems 3730 DNA Analyzer. The assembled contig sequence was deposited in GenBank under accession number KF586842.

Molecular phylogenetic analysis

Ribosomal DNA sequences of x-51 were aligned with 113 OTUs from zoosporic fungi and closely related uncultured clones collected from the GenBank database. Sequences were selected based on the following scheme. First, all chytrid LSU genes that had sufficiently large length (> 2 000 bp) were added to the list of OTUs, and SSU genes were selected for all listed species. Second, all fragments of chytrid SSU and LSU rRNA genes were selected from cultured strains and environmental samples that occupied isolated positions on the distance tree. Third, all sequences of uncultured clones available in GenBank as of January 2013 were selected that grouped closely with x-51 CALU and *Mesochytrium penetrans* x-10 CALU. For environmental sample sequences that formed particularly long branches on the distance tree we performed an additional

Rhizophidiales

1.0|60 *Rhizophydium* sp. JEL316 AFTOL-ID 1535
1.0|81 *Rhizophlyctis harderi* JEL171 AFTOL-ID 31
1.0|65 *Rhizophydium brooksianum* JEL136 AFTOL-ID 22
Rhizophydium sp. JEL317 AFTOL-ID 35
0.97|84 *Boothiomyces macroporosum* AFTOL-ID 689
0.99|46 *Kappamyces laurelensis* AFTOL-ID 690
Rhizophydium sp. JEL151 AFTOL-ID 30
Rhizophydium sphaerotheca AFTOL-ID 37
1.0|92 *Entophlyctis* sp. JEL174 AFTOL-ID 38
Entophlyctis sp. DU-DC1 AF164255
Entophlyctis helioformis JEL326 AFTOL-ID 40
Batrachochytrium dendrobatidis AAHL-97-845 AFTOL-ID 21
Homoloaphlyctis polyrhiza JEL142

0.67|35

0.59|42

Spizellomycetales

0.99|66 *Spizellomyces punctatus* AFTOL-ID 182
Powellomyces sp. JEL95 AFTOL-ID 32
0.99|83 *Triparticalcar arcticum* AFTOL-ID 696
0.88|56 *Gaertneriomyces semiglobiferus* AFTOL-ID 34

Rhizophlyctidales

0.73|40 *Catenomyces* sp. JEL342 AFTOL-ID 47
Rhizophlyctis rosea AFTOL-ID 43
0.71|50 *Blyttiomyces helicus* AFTOL-ID 2006
P34.43 AY642701

0.57|15

Chytridiales

1.0|93 *Podochytrium dentatum* AFTOL-ID 1539
Chytriomyces sp. JEL378 AFTOL-ID 1532
Rhizoclosmatium sp. JEL347-h AFTOL-ID 20
Chytriomyces spinosus AFTOL-ID 1540
Chytridiales sp. JEL187 AFTOL-ID 39
1.0|87 *Chytriomyces* sp. WB235A AFTOL-ID 1536
0.62|67 *Chytriomyces hyalinus* AFTOL-ID 1537
Chytridium sp. JEL341 AFTOL-ID 1531
Rhizophydium sp. JEL221 AFTOL-ID 1534
Phlyctochytrium planicorne AFTOL-ID 628
Rhizophydium sp. JEL354 AFTOL-ID 41

0.87|30

Cladochytriales

0.98|64 *Nowakowskiella* sp. JEL127 AFTOL-ID 146
Endochytrium sp. JEL324 AFTOL-ID 631
Diplochytridium lagenarium JEL72
1.0|86 *Nephrochytrium* sp. JEL125
Cladochytrium replicatum
Endochytrium sp. JEL325

0.57|10

Polychytriales

Karlingiomyces asterocystis JEL572
Arkaya lepida JEL93 AFTOL-ID 629
0.79|19 *Neokarlingia chitinophila* JEL510
Lacustromyces hiemalis JEL31
1.0|70 *Polychytrium aggregatum*

Lobulomycetales

Chytridiales sp. PL70 EF443143
0.94|55 *Lobulomyces angularis* AFTOL-ID 630
0.97|52 *Maunachytrium keaense* AF021 EF432822.2
CCW64 AY180029
Chytridiales sp. AF011 EF432819.2
RSC-CHU-20 AJ506002
IIS1-20 EU517013
0.53|33 D2P03D7 EF100268
AY2009B4 HQ219419
FV23_1H5 DQ310332

0.61|24

0.58|31

0.69|35

Mesochytriales

0.4|62 WS 10-E02 AJ867629
WS 10-E15 AJ867631
WS 10-E14 AJ867630
0.52|33 Spring-37 JX069054
T2P1AeF04 GQ995412
SAPA5_E7 FJ483310
0.63|41 T2P1AeB05 GQ995415
P60E-29 DQ104068
P60E-9 DQ104060
0.59|52 T3P1AeC03 GQ995413
◄ 7 clones from a lake in China
T5P2AeC07 GQ995414
PFA12SP2005 EU162643
1.0|75 PFD6SP2005 EU162637 3'-end
Pa2007C10 JQ689425
0.4|66 ◄ 20 clones from Lake Bourget
1.0|82 PFF5SP2005 EU162641
F08_SE1B FJ592495 3'-end
Mesochytrium penetrans CALU x-10
1.0|75 ThJAR2B-48 JF972676
528-O25 EF586095
0.72|98 Spring-57 JX069067
Spring-71 JX069077
Spring-08 JX069031
0.69|42 GA069 HM486988
GF29312 JX417945
0.63|28 PA2009E7 HQ191286
Va2007BB6 JQ689445
1.0|86 PA2009B6 HQ191400
1.0|77 PA2009D8 HQ191406
PA2009C3 HQ191369
PFG9SP2005 EU162638

0.98|69

0.83|53

1.0|82

Gromochytriales

0.73|09 kor_110904_17 FJ157331
IIN1-34 EU516964
0.95|62 *Gromochytrium mamkaevae* CALU x-51

Synchytriaceae

OTU97-188 JQ310927
OTU97-621 JQ311409
Synchytrium endobioticum P-58, Sluknov
0.76|71 *Synchytrium endobioticum* AS1
Synchytrium decipiens AFTOL-ID 634
1.0|94 *Synchytrium macrosporum* AFTOL-ID 635

incertae sedis

LLSG10_1 PML-2011t JN049552
0.82|98 18s3-24 EU733608
18s1-47 EU733554

Monoblepahridomycetes

1.0|85 L73_ML_156 FJ354068
PFE7AU2004 DQ244008
0.99|64 Elev_18S_563 EF024210
Hyaloraphidium curvatum AFTOL-ID 26
1.0|92 *Oedogoniomyces* sp. CR84
Monoblepharella mexicana AFTOL-ID 33
Gonapodya prolifera

Neocallimastigomycota

D3 EU910609
Cyllamyces aberensis AFTOL-ID 846
1.0|79 *Orpinomyces* sp. OUS1
Neocallimastix sp. AFTOL-ID 638

Blastocladiomycota

Physoderma maydis AFTOL-ID 19
Blastocladiella emersonii
Allomyces arbusculus AFTOL-ID 300

0.69|53

0.72|30

outgroup

Rozella sp. JEL347 AFTOL-ID 16
Rozella allomycis AFTOL-ID 297
Amoeboaphelidium protococcarum CALU x-5

0.05

Fig. 2 Bayesian phylogenetic tree based on concatenated rDNA sequences (18S, 5.8S, 28S). Node support values are given by Bayesian posterior probability (left of the vertical line) and Maximum Likelihood bootstrap support (right of the vertical line). Support values are omitted for nodes that score above 95 % in both analyses (edges drawn with thick lines) and nodes that score less than 50 % in both analyses (edges drawn with striated lines). The strain x-51 - *Gromochytrium mamkaevae* is highlighted with red. Two groups of nearly identical clones in the *Mesochytriales* clade are collapsed into single branches (represented by triangles).

verification step that involved breaking the sequence into two or more non-overlapping fragments that were then used as independent OTUs for preliminary phylogenetic analysis (data not shown). This method identified seven sequences (accession numbers: EU162637, EF196798, EF196785, EF196773, EF196750, FJ592495, HQ191339) from three independent environmental samples as potentially chimaeric. The parts of sequences EU162637 and FJ592495 that presumably have fungal source were retained; the remainder and the other four sequences were excluded from the phylogenetic analysis. To minimise missing data a small number of sequences was assembled by fusing or constructing a consensus of sequences from different isolates of the same species or by fusing partial sequences that have a 98–100 % overlap identity. The full list of consensus and chimaeric sequences constructed for the purpose of phylogenetic analysis is presented in Table 1 and Fig. 2. The sequences of early-branching fungal taxa – *Rozella allomycis* and *Amoeboaphelidium protococcarum* were chosen

Table 2 List of environmental clones of the *Mesochytriales* and *Gromochytriales*.

Name	GenBank accession no.	Habitat / Geographic location	Characterisation / Season	Reference
Gromochytrium mamkaevae CALU x-51	KF586842	Ditch near town Kirovsk, Leningrad Region	parasite of yellow-green alga *Tribonema gayanum*	This paper
Mesochytrium penetrans CALU x-10	FJ804149; FJ804153	Small lake in Karelia (Northern Europe)	parasite of green alga *Chlorococcum minutum*	Karpov et al. (2010)
528-O25	EF586095	Opanuku Stream biofilm, Auckland, New Zealand		Dopheide et al. (2008)
PFD6SP2005, PFG9SP2005, PFF5SP2005, PFA12SP2005	EU162637, EU162638, EU162641, EU162643	Oligo-mesotrophic mountain Lake Pavin, France	May – June	Lefèvre et al. (2008)
BI74, B1, B43, B44, B46-138, B49, B52, B56, BI78, BI88, BI100, BI104, BI107, BI121, BI123, BI15, BI72, BI76, B86-161, BI5	EF196711, EF196713, EF196728, EF196729, EF196731, EF196734, EF196735, EF196738, EF196745, EF196749, EF196751, EF196753, EF196755, EF196762, EF196763, EF196765, EF196775, EF196776, EF196786, EF196799	Large mesotrophic alpine Lake Bourget, France	May – August	Lepère et al. (2008)
F08_SE1B	FJ592495	Cold-fumarole soil, Socompa Volcano, Andes (elev. 5824 m)	April	Costello et al. (2009)
P60E-9, P60E-29	DQ104060, DQ104068	Glacial ice from Tibetan plateau	150-yr-old ice	Zhang et al. (2009)
T2P1AeB05, T2P1AeF04, T3P1AeC03, T5P2AeC07	GQ995415, GQ995412, GQ995413, GQ995414	High-elevation soil not far from ice and snow	July – October	Freeman et al. (2009)
PA2009C3, PA2009B6, PA2009D8, PA2009E7	HQ191369, HQ191400, HQ191406, HQ191286	Oligo-mesotrophic mountain Lake Pavin, France	July	Monchy et al. (2011)
SAPA5_E7	FJ483310	Salt marsh, USA: RI	Summer	Mohamed & Martiny (2011)
ThJAR2B-48	JF972676	Air sample, Greece	October	Genitsaris (2011)
GA069	HM486988	Feces from a detritus-feeding crustacean *Gammarus tigrinus*; Canada	September – October	Sridhar et al. (2011)
Spring_08, Spring_37, Spring_57, Spring_71	JX069031, JX069054, JX069067, JX069077	River site, Southern Alberta, Canada	Spring	Thomas et al. (2012)
Pa2007C10	JQ689425	Oligo-mesotrophic mountain Lake Pavin, France	April	Jobard et al. (2012)
Va2007BB6	JQ689445	Large brown-coloured humic and mesotrophic Lake Vassivière, France	May	Jobard et al. (2012)
WS 10-E02, WS 10-E14, WS 10-E15	AJ867629, AJ867630, AJ867631	Melted white snow water, alpine Lake Joeri XIII, Switzerland	–	Unpubl. data
GF29312	JX417945	Greenhouse soil, China	–	Unpubl. data
Seven clones from a freshwater lake in China	JX426910, JX426918, JX426923, JX426937, JX426998, JX427002, JX427011	Freshwater lake, China	–	Unpubl. data
kor_110904_17	FJ157331	Lake Koronia water column, Greece	Nov.	Genitsaris et al. (2009)
IIN1-34	EU516964	Alpine snow-covered soil, Alpes, Austria	–	Unpubl. data
Nineteen clones: E109_XXX, E107_XXX	KC561936–KC561954	High mountain soil Nepal	October	Naff et al. (2013)
Five clones: R11a_XX	KC561955–KC561959	Rocky Mountain talus snow, Colorado, USA	July – August	Naff et al. (2013)
Sixteen clones: d̄31a_XX, T31b_XX	KC561960–KC561975	Rocky Mountain talus snow, Colorado, USA	July – August	Naff et al. (2013)
NKS146	JX296576	Hyposaline soda lake Nakuru, Kenya, East Africa	November	Luo et al. (2013)

as outgroup (James et al. 2006, Karpov et al. 2013). Alignments were generated with MUSCLE (Edgar 2004) and refined manually using BioEdit (Hall 1999). After discarding ambiguously aligned nucleotide positions and concatenating the alignments of 18S, 5.8S and 28S rRNA genes, the alignment consisted of 4 850 positions. Tree search for the concatenated alignment was performed using the Bayesian method implemented by MrBayes v. 3.1.2 (Ronquist & Huelsenbeck 2003). The tree reconstruction used GTR+G12+I model and partition by genes (18S, 5.8S, and 28S) with all parameters unlinked, except the topology and branch lengths. Four independent runs of eight Markov Chain Monte Carlo (MCMC) were performed to evaluate the convergence. Chains were run for 10 million generations sampling trees every 1 000 generations after discarding the first 8 million as burn-in. Sampled trees were used to generate a majority rule consensus tree with Bayesian posterior probabilities. Bootstrap support values for the consensus tree reconstructed by MrBayes were generated using RAxML v. 7.2.6 (Stamatakis 2006) on the basis of 1 000 replicates under the GTR+G+I model.

RESULTS

Light microscopy

The parasite has a typical chytrid endogenous life cycle with tiny (~ 2 µm diam) zoospores that attach to the host cell surface, retract the flagellum and encyst. After the germ tube enters the host the zoospore cyst enlarges; a prominent lipid globule is clearly visible at this early stage (Fig. 1a). The young sporangium has homogenous contents with few lipid globules of different size (Fig. 1b), and the mature sporangium contains zoospores, which are released through an apical pore. The inoperculate sporangium is long ovoid (~ 18 × 10 µm diam) without a differentiated apical papilla (Fig. 1c). The apical pore varies in its dimensions: from narrow to as broad as the diameter of the sporangium or even broader (Fig. 1e). The delicate rhizoidal system is poorly visible, but can be estimated as weakly branched with short rhizoids emerging from a slender main axis (Fig. 1d, e). According to this description the fungus could be identified as *Rhizophydium mammillatum* (A. Braun) A. Fish. (1892) or, less likely, *R. melosirae* (1952) (Sparrow 1960, Letcher & Powell 2012), and therefore it was identified as *R. mammillatum* (Mamkaeva et al. 2006).

Molecular phylogeny

The rDNA sequences of strain x-51 occupy an isolated position in the tree (Fig. 2); its closest relatives are three uncultured clones: one from Lake Koronia in Greece (clone kor_110904_17), another from snow-covered soil in alpine Austria (clone IIN1-34), and one more from a hyposaline soda lake in Kenya, East Africa (Genitsaris et al. 2009, Kuhnert et al. 2012, Luo et al. 2013). Together these sequences form a new phylogenetic group. Among the described organisms, the closest relative of this group is *Mesochytrium penetrans*, which was classified in the *Chytridiomycetes incertae sedis* (Karpov et al. 2010). *Mesochytrium penetrans* is the only described species of a diverse group of uncultured fungi from soil, freshwater and hydrobiont gut samples collected from temperate zone of Eurasia and North America (Table 2). This group was recognised earlier as an order-level 'Novel clade I' within the *Chytridiomycetes* (Lefèvre et al. 2008, Jobard et al. 2012). Another name for 'clade I' is 'snow chytrids' ('Snow Clade 1' or SC1) according to Naff et al. (2013). The rDNA data places the clade uniting x-51 and the 'clade I' (Lefèvre et al. 2008) sister to *Lobulomycetales* (Simmons et al. 2009), albeit with relatively low support (Fig. 2). The distances inside the clusters of OTUs that contain x-51 and *M. penetrans* on the rDNA tree are comparable to the distances inside the established orders of *Chytridiomycota*, and distances between the OTUs in these clusters and the members of *Lobulomycetales* are no less than the distances between different orders of *Chytridiomycota* (Fig. 2).

Zoospore ultrastructure

The spherical zoospore has a posterior flagellum and sometimes produces short anterior filopodia (Fig. 3c). A core of aggregated ribosomes is located in the posterior part of the cell. The ribosomal aggregation is relatively small and does not have surrounding endoplasmic reticulum (Fig. 3, 4). The ribosomes fill the space between the flagellar base and the nucleus and have no connection with nucleus, mitochondria or other membrane bounded organelles.

Several mitochondria with flat cristae reside at the cell periphery. A nearly central nucleus associates with anteriorly adpressed narrow microbody and a single large lipid globule anteriorly attached to the microbody (Fig. 3a). The anterior flat side of the lipid globule is bounded by a prominent fenestrated cisterna (rumposome) oriented to the cell exterior. Thus, the microbody-lipid globule complex (MLC) contains a single microbody enveloping a large anterior lipid globule with fenestrated cisterna.

Endoplasmic reticulum cisternae are rare and are normally found at the cell periphery. A vesicle rich zone occupies an area from one side of the ribosomal core extending from the nucleus to the centriole (Fig. 3a, c). Several small vesicles with electron-opaque contents (dense bodies) are present in the cytoplasm of the anterior part of the cell.

Kinetid structure

The structure of the flagellar apparatus was investigated with serial sections of six released zoospores. The kinetosome and centriole are embedded in the ribosomal core (Fig. 3d, e, 4). The kinetosome is c. 400 nm long and composed of microtubular doublets (not triplets) with developed transitional fibers (props) (Fig. 4b–d). The flagellar transition zone is simple without transversal plate, but with a slightly inward curved diaphragm at the distal end of kinetosome (Fig. 4g). Two thin lines parallel to the peripheral microtubular doublets are present above the diaphragm, and seem to correspond to the spiral fiber, or cylinder (Fig. 4g). The centriole is about 100 nm long and lies at an angle of c. 30° to the kinetosome (Fig. 3e, 4b, c, e, f). The kinetosome is connected to the centriole by a broad fibrillar bridge composed of at least three thick connectors (Fig. 4d). The longest middle connector passes through the bottom of kinetosome to the side of centriole. The structure of interconnecting bridge seems to be an unstable character. The bridge looks rather broad and prominent, connecting the sides of kinetosome and centriole at the longitudinal sections (Fig 4e, f), but it is not visible at the corresponding transverse sections (Fig. 4b–d). Approximately 1/3 of all serial sections had the broad bridge connecting the sides of kinetosome and centriole and in 2/3 of the series the bridge connects the bottom of kinetosome to the side of centriole. The diagram (Fig. 5a) shows the more common state.

The kinetosome produces at least two microtubular roots. The anterior root consists of two microtubules and passes laterally in the direction of the lipid globule crossing the surface of fenestrated cisterna (Fig. 3a, 5). The posterior root is much shorter, composed of one or two microtubules and is directed right about the anterior root (Fig. 4a–d). Their origin is not clear: anterior root emerges in the vicinity of kinetosome, and posterior root appears somewhere in between the kinetosome and the centriole.

One more kinetosomal derivate, a spur, lies close to the outer surface of the kinetosome on the side opposite the centriole
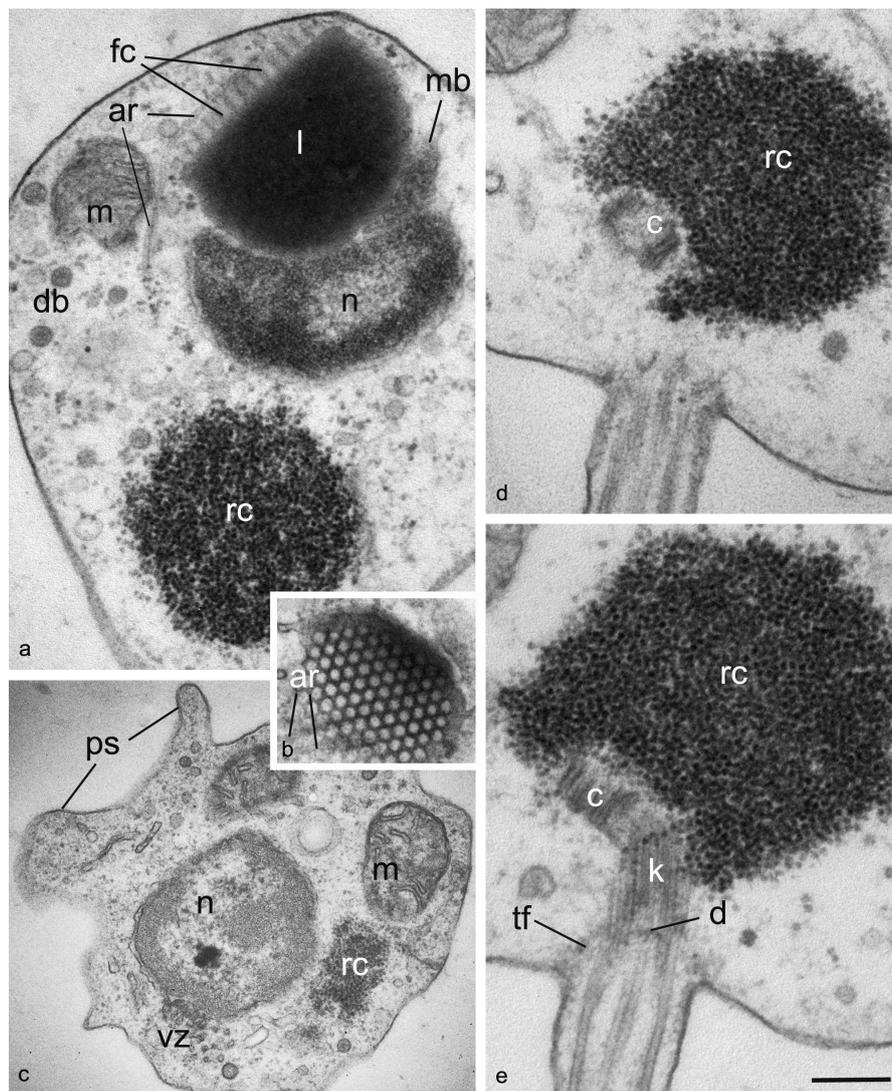
Fig. 3 General ultrastructure of *Gromochytrium mamkaevae* (x-51 CALU) zoospore. — a. General disposition of nucleus and other organelles at LS; b. tangential section of fenestrated cisterna crossed by anterior microtubular root; c. pseudopodia at cell anterior; d, e. two consecutive sections of the kinetid. — Abbreviations: ar = anterior microtubular root; c = centriole; d = kinetosome diaphragm; db = dense bodies; fc = fenestrated cisterna; k = kinetosome; l = lipid globule; m = mitochondrion; mb = microbody; n = nucleus; ps = pseudopodia; rc = ribosomal core; tf = transitional fibers (props); vz = vesicular zone. — Scale bar on E: a = 300 nm; b, c = 400 nm; d, e = 200 nm.

(Fig. 4f, g). The spur is thin and short, projecting about 70–100 nm from the kinetosome into the ribosomal core (Fig. 4f).

A general scheme of zoospore ultrastructure is illustrated in Fig. 5a.

DISCUSSION

According to the morphology of strain x-51 at different life cycle stages it belongs to the genus *Rhizophydium* sensu Sparrow (1960). It has a simple thallus composed of inoperculate monocentric epibiotic elongated sporangium. It bears a single slightly branching rhizoidal axis. Judging by the shape of the sporangium and its dimensions this strain could be *Rh. mammillatum*, however, contrary to *Rh. mammillatum*, the sporangium of x-51 has no papilla. Our study has shown that zoospore ultrastructure of x-51 differs cardinally from that of *Rhizophydium* and other members of *Rhizophydiales* (Letcher et al. 2006, 2008). The order *Rhizophydiales* has 18 zoospore types that are rather different from each other, but none have a posterior ribosomal core without delimiting ER and mitochondria separated from MLC as in x-51. The MLC structure in the zoospore of x-51 has similarities with that of the recently established *Gorgonomyces*, which unlike other rhizophydiales has a close association of nucleus with microbody and lipid globule

(Letcher et al. 2008), but in all other respects the zoospore of *Gorgonomyces* is different.

Molecular phylogeny places the strain x-51 far from *Rhizophydiales*, as a sister to 'clade I' – a cluster containing many environmental sequences of the *Chytridiomycetes* (Lefèvre et al. 2008, Jobard et al. 2012) besides a formally described species *Mesochytrium penetrans*, which was earlier shown to have a rather isolated position among the *Chytridiomycetes* (Karpov et al. 2010). The features that distinguish *Mesochytrium* are the partial penetration of the host cell by the sporangium and a zoospore with a unique ultrastructural organization.

Thus, we have to compare the zoospore structure of strain x-51 with that of *M. penetrans.* Two strains of *M. penetrans* (x-10 and x-46 CALU) were studied by electron microscopy, and 18S and 28S rRNA genes were sequenced for x-10 (Gromov et al. 2000, Karpov et al. 2010). Their general organization differs from that of x-51; unlike x-51 the *M. penetrans* has no ribosomal aggregation, its mitochondrion with MLC is enclosed by ER, a fenestrated cisterna faces the posterior of the cell, and a vacuole is present (Fig. 5b). At the same time, some morphological characters are similar in x-51 and x-10; both have small dense vesicles in the cytoplasm, which are common for the *Chytridiomycetes*; the kinetosomes lie at the same angle to each other and the flagellar transition zones contain a spiral
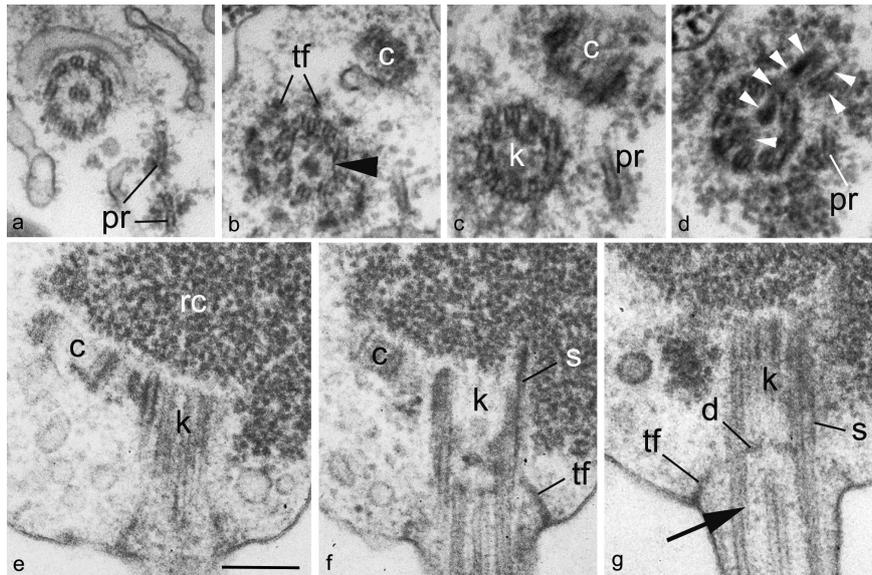
Fig. 4 Kinetid structure of *Gromochytrium mamkaevae* (x-51 CALU) zoospore. a–d. Selected serial TS of the kinetid from distal to proximal. View from flagellar base to top. Arrowhead on b shows a spiral fiber. Arrowheads on d mark the bridge between kinetosome and centriole; e–g. selected serial LS of the kinetid. Arrow on g shows a spiral fiber. — Abbreviations: c = centriole; d = kinetosome diaphragm; k = kinetosome; pr = posterior microtubular root; rc = ribosomal core; s = spur; tf = transitional fibers (props). — Scale bar on E: a–d = 300 nm, e–g = 200 nm.

element or a cylinder (Fig. 5). The kinetid structure also has some differences; x-51 has two microtubular roots which are absent in *M. penetrans*, a bridge in x-51 connects the bottom of kinetosome to the lateral surface of the centriole, not the lateral surfaces of kinetosome and centriole as in *M. penetrans* and the kinetosome of x-51 is composed of microtubular doublets. The spur structure and shape are also different; in x-51 the spur is inconspicuous and straight and in *M. penetrans* it is long and curved enclosing both the kinetosome and the centriole (Fig. 5).

We conclude, that the overall organization and kinetid structure of the zoospores of *M. penetrans* and x-51 differ considerably. According to the modern paradigm stemming from D. Barr's studies (e.g. Barr 1978, Barr & Hadland-Hartmann 1978, Powell 1978, Longcore 1995, 1996, Letcher et al. 2006, 2008, Simmons 2009), their zoospores certainly have enough peculiarities to separate them at the taxonomic level of order. Moreover, their zoospores can be regarded as having a unique organization among the chytridiomycetes. We have already shown this for *M. penetrans* (Karpov et al. 2010). For the strain x-51 the unique characters are: the posterior core of ribosomes is not bounded by ER membranes, mitochondria are not associated with MLC, and a bridge connects the bottom of kinetosome to centriole.

The nearest branch to the x-51/*Meshochytrium* cluster is the order *Lobulomycetales* (Fig. 2), a group that was recently established on the basis of SSU and partial LSU gene phylogeny and ultrastructural analysis of zoospores (Simmons et al. 2009). In the previous study, the 18S and 28S sequences of *M. penetrans* (strain x-10 CALU) also placed this strain as a sister lineage to *Lobulomycetales* but with a rather low support (Karpov et al. 2010). 'Snow chytrids' were also suggested as a deep divergent branch sister to *Lobulomycetales* (Naff et al. 2013). In the present study the increased taxon sampling through the addition of environmental sequences results in better support for the sister group position of the x-51/*Meshochytrium* cluster relative to *Lobulomycetales* (Fig. 2).

Zoospores of *Lobulomycetales* (*Lobulomyces angularis*, *Clydaea vesicula* and *Maunachytrium keaense*) differ from those of x-51 and *Meshochytrium* in a number of ways: kinetids of lobulomycetes have parallel centrioles, an electron-opaque plug is present in the flagellar transition zone, and no spur or flagellar roots are found; the ribosomal core in *Lobulomycetes*

is bounded by the ER, and the vacuole and 1–2 lipid globules lie posteriorly (Simmons et al. 2009). The presence of a rumposome (fenestrated cisterna) was noted in the text, but not shown in the pictures of the above cited article, therefore its precise position is unknown for *Lobulomycetales*.

Thus, our morphological data strongly support an isolated position of x-51/*Meshochytrium* cluster on the phylogenetic tree.

Taxonomy

An isolated position of *Mesochytrium* was shown by 18S+28S rRNA gene phylogeny and zoospore morphology of two strains: x-46 CALU (Gromov et al. 2000) and x-10 (Karpov et al. 2010), and recapitulated by molecular phylogenetic analysis in the present paper. The sequence of *M. penetrans* clusters with a large number of environmental sequences forming a clear monophyletic branch with good statistical support (Fig. 2). Molecular phylogenetic analysis of this genus does not reveal family or ordinal level affinity of *M. penetrans*, consequently in the previous paper we referred to it as *incertae sedis* (Karpov et al. 2010). Here we have a better resolved tree with a number of environmental sequences and a new neighbour of this branch that includes isolate x-51. Because of the molecular phylogeny of *M. penetrans* and CALU x-51, together with each having a unique organisation of zoospores, we establish new orders and families for both, plus a new genus and species for CALU x-51.

Gromochytriales Karpov & Aleoshin, *ord. nov*. — MycoBank MB805305

Zoospore with posterior ribosomal aggregation not bounded by endoplasmic reticulum. Microbody-lipid complex adpressed to the nucleus and containing a single microbody enveloping a large anterior lipid globule with anteriorly oriented fenestrated cisterna. Several mitochondria are separated from MLC. Small dense bodies present in peripheral cytoplasm. Kinetosome and centriole embedded in posterior side of the ribosomal core. *Flagellar transition zone* contains a spiral fiber, or a cylinder. Centriole at an angle of c. 30° to kinetosome; bottom of kinetosome connected by a broad fibrillar bridge to centriole. Anterior and posterior microtubular roots and a short straight spur associated with kinetosome.
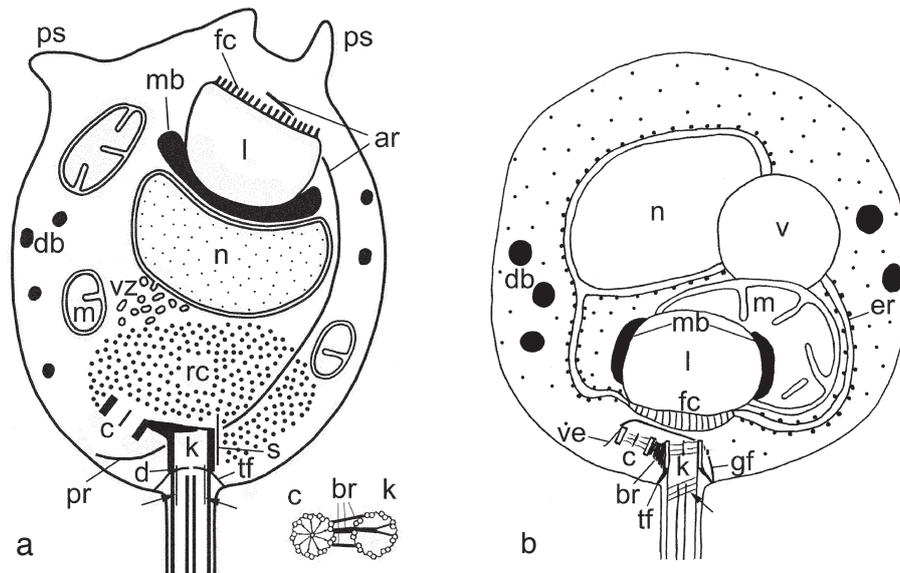
Fig. 5 General scheme of zoospore structure. — a. *Gromochytrium mamkaevae* (x-51 CALU); b. *Mesochytrium penetrans* (x-10 CALU). Arrows show the spiral fiber in flagellar transition zone (b: after Karpov et al. (2010) with modified abbreviations).— Abbreviations: ar = anterior microtubular root; br = bridge between kinetosome and centriole; c = centriole; d = kinetosome diaphragm; db = dense bodies; er = endoplasmic reticulum; fc = fenestrated cisterna; gf = girdle fiber; k = kinetosome; l = lipid globule; m = mitochondrion; mb = microbody; n = nucleus; pr = posterior microtubular root; ps = pseudopodia; rc = ribosomal core; s = spur; tf = transitional fibers (props); v = vacuole; ve = veil; vz = vesicular zone.

Gromochytriaceae Karpov & Aleoshin, *fam. nov*. — MycoBank MB805306

Type genus. Gromochytrium Karpov & Aleoshin.

Description as for *Gromochytriales*: simple thallus with inoperculate, monocentric, epibiotic sporangium having endogenous development and single slightly branching rhizoidal axis.

Gromochytrium Karpov & Aleoshin, *gen. nov*. — MycoBank MB805307

Type species. Gromochytrium mamkaevae Karpov & Aleoshin.

Simple thallus with inoperculate, monocentric, epibiotic sporangium having endogenous development and single slightly branching rhizoidal axis. *Zoospore* with posterior ribosomal aggregation unbounded by endoplasmic reticulum. Microbody-lipid-complex adpressed to the nucleus and contains a single microbody enveloping a large anterior lipid globule with anteriorly oriented fenestrated cisterna. Several mitochondria are separated from MLC. Small dense bodies present in peripheral cytoplasm. Kinetosome and centriole embedded in posterior side of the ribosomal core. *Flagellar transition zone* contains a spiral fiber, or a cylinder. Centriole at an angle of c. 30° to kinetosome; bottom of kinetosome connected by a broad fibrillar bridge to centriole. Anterior and posterior microtubular roots and a short straight spur associated with kinetosome composed of microtubular doublets.

Gromochytrium mamkaevae Karpov & Aleoshin, *sp. nov*. — MycoBank MB805308, GenBank KF586842; Fig. 1–5a

Etymology. Genus named in honour of Boris V. Gromov, a prominent Russian microbiologist, and species named in honour of his spouse, colleague and co-author, Kira A. Mamkaeva.

Mature inoperculate epibiotic sporangium long ovoid (18 × 10 µm) without papillae. *Zoospores* released through apical pore. Delicate, weakly branched rhizoidal system with short rhizoids emerging from a slender main axis. *Zoospores* 2 µm diam with single lipid globule.

Specimen examined. Russia, Leningrad Region, ditch near town Kirovsk, parasite of *Tribonema gayanum.* Holotype x-51 presented by fixed specimen embedded in resin block for electron microscopy. Deposited in CALU (Biological Faculty of St. Petersburg State University, St. Petersburg 199034, Russia).

Mesochytriales Karpov & Aleoshin, *ord. nov.* — MycoBank MB805303

Zoospores with unique ultrastructural organisation; centriole at an angle of c. 30° to kinetosome; ribosomes dispersed through the cytoplasm; mitochondrion and MLC surrounded by rough endoplasmic reticulum.

Mesochytriaceae Karpov & Aleoshin, *fam. nov.* — MycoBank MB805304

Description as for *Mesochytriales*. Sporangium inoperculate, monocentric, epibiotic, endogenous, semi absorbed by host cell.

Mesochytrium B.V. Gromov, Mamkaeva & Pljusch. Nova Hedwigia 71: 159. 2000, emend. Karpov

Type species. Mesochytrium penetrans B.V. Gromov, Mamkaeva & Pljusch.

Zoosporangium sessile, partially penetrating host cell. Delicate branched rhizoids emerge near the sporangial base. *Zoospores* spherical to oval with single lipid globule and dispersed ribosomes. Microbody-lipid-complex composed of a single mitochondrion and a single lipid globule partially covered with microbody and posterior fenestrated cisterna; centriole with veil at an angle of c. 30° to kinetosome, the two being connected by a broad, dense fibrillar bridge. *Flagellar transition zone* contains a spiral fiber. *Resting spore* endobiotic, spherical with smooth thick wall.

Mesochytrium penetrans B.V. Gromov, Mamkaeva & Pljusch. Nova Hedwigia 71: 159. 2000, emend. Karpov

Sporangium pyriform 10–14 × 6–7.5 µm with thin smooth wall and apical papilla. *Zoospores* spherical 2–2.5 µm diam with

a 5–14 µm long flagellum. Parasite of green alga *Chlorococcum minutum.*

Specimen examined. Small lake Pryazha in Karelia, parasite of *Chlorococcum minutum.* Holotype CALU x-46.

Diversity and abundance of *Mesochytriales* and *Gromochytriales* in nature

The fact that *Mesochytrium penetrans* and *Gromochytrium mamkaevae* have thus far not been found during environmental DNA studies indicates that these species are not prevalent in the sampled ecosystems, at least not during the time of sampling. This fact emphasizes the incompleteness of our current knowledge of chytrid diversity and the importance of collecting new samples for exhaustive description of fungal diversity. At the same time, some of the undescribed species from the *Mesochytriales* clade that are represented by almost identical clones were repeatedly recovered in several environmental samples. Such clusters are formed by clones shown on Fig. 2 as small black triangles: one is presented by PFG9SP2005, PA2009C3, PA2009B6, PA2009D8 (Lefèvre et al. 2008, Monchy et al. 2011), another by PFF5SP2005, PFD6SP2005 (3'-end), Pa2007C10 and 20 clones are from Lake Bourget (Lefèvre et al. 2008, Lepère et al. 2008, Jobard et al. 2012), collected during the course of several years from lakes in France. Moreover, the clones of *Mesochytriales* from Lake Bourget form a substantial fraction of all fungal clones in the sample, which implies that their zoospores were ubiquitous during the time of sampling. It is likely that the abundance of *Mesochytriales* may vary by season. Ribosomal DNA clones of *Mesochytriales* accounted for about 50 % of the number of fungal rDNA clones from Lake Pavin (France) in spring and summer seasons (Lefèvre et al. 2008, Jobard et al. 2012), but they were not detected there in autumn (Lefèvre et al. 2007). Similarly to *M. penetrans* and *G. mamkaevae*, these clones probably can be attributed to parasites of algae. The diversity and abundance of rDNA clones from undescribed members in these environmental samples suggest that members of the *Mesochytriales* may play an important role as regulators of phytoplankton populations (Lefèvre et al. 2008, Lepère et al. 2008, Genitsaris et al. 2009, Monchy et al. 2011).

REFERENCES

Auwera G van der, Chapelle S, Wachter R de. 1994. Structure of the large ribosomal subunit RNA of Phytophthora megasperma, and phylogeny of the oomycetes. FEBS Letters 338: 133–136.

Barr DJS. 1978. Taxonomy and phylogeny of Chytrids. BioSystems 10: 153–162.

Barr DJS, Hadland-Hartmann VE.1978. Zoospore ultrastructure in the genus Rhizophydium (Chytridiales). Canadian Journal of Botany 56: 2380–2404.

Costello EK, Halloy SR, Reed SC, Sowell P, Schmidt SK. 2009. Fumarole-supported islands of biodiversity within a hyperarid, high-elevation landscape on Socompa Volcano, Puna de Atacama, Andes. Applied and Environmental Microbiology 75: 735–747.

Dopheide A, Lear G, Stott R, Lewis G. 2008. Molecular characterization of ciliate diversity in stream biofilms. Applied and Environmental Microbiology 74: 1740–1747.

Edgar RC. 2004. MUSCLE: multiple sequence alignment with high accuracy and high throughput. Nucleic Acids Research 32: 1792–1797.

Freeman KR, Martin AP, Karki D, Lynch RC, Mitter MS, et al. 2009. Evidence that chytrids dominate fungal communities in high-elevation soils. Proceedings of the Natural Academy of Sciences USA 106: 18315–18320.

Genitsaris S. 2011. Airborne microorganisms in urban areas: biodiversity, succession and dispersion. PhD thesis, Aristotle University of Thessaloniki, Greece (in Greek). http://invenio.lib.auth.gr/record/128157/files/GRI-2011-7695.pdf?version=1.

Genitsaris S, Kormas KA, Moustaka-Gouni M. 2009. Microscopic eukaryotes living in a dying lake (Lake Koronia, Greece). FEMS Microbiology Ecology 69: 75–83.

Gromov BV, Mamkaeva KA, Pljusch AV. 2000. Mesochytrium penetrans gen. et sp. nov. (Chytridiales) – a parasite of the green algae Chlorococcum minutum (Chlorococcales), with an unusual behaviour of the sporangia. Nova Hedwigia 71: 151–160.

Gromov BV, Titova NN. 1991. CALU-collection of algal cultures in the laboratory of microbiology of Biological Institute of Sankt-Petersburg University. In: Catalogue of microalgal cultures in the collections of the USSR: 76–125. RAS, Moskow.

Hall TA. 1999. BioEdit: a user-friendly biological sequence alignment editor and analysis program for Windows 95/98/NT. Nucleic Acids Research S41: 95–98.

James TY, Letcher PM, Longcore JE, Mozley-Standridge SE, Porter D, Powell MJ, Griffith GW, Vilgalys R. 2006. A molecular phylogeny of the flagellated fungi (Chytridiomycota) and description of a new phylum (Blastocladiomycota). Mycologia 98: 860–871.

James TY, Porter D, Leander CA, Vilgalys R, Longcore JE. 2000. Molecular phylogenetics of the Chytridiomycota supports the utility of ultrastructural data in chytrid systematics. Canadian Journal of Botany 78: 336–350.

Jobard M, Rasconi S, Solinhac L, Cauchie HM, Sime-Ngando T. 2012. Molecular and morphological diversity of fungi and the associated functions in three European nearby lakes. Environmental Microbiology 14: 2480–2494.

Karpov SA, Letcher PM, Mamkaeva MA, Mamkaeva KA. 2010. Phylogenetic position of the genus Mesochytrium (Chytridiomycota) based on zoospore ultrastructure and 18S and 28S rRNA gene sequences. Nova Hedwigia 90: 81–94.

Karpov SA, Mikhailov KV, Mirzaeva GS, Mirabdullaev IM, Mamkaeva KA, Titova NN, Aleoshin VV. 2013. Obligately phagotrophic aphelids turned out to branch with the earliest-diverging Fungi. Protist 164: 195–205.

Kuhnert R, Oberkofler I, Peintner U. 2012. Fungal growth and biomass development is boosted by plants in snow-covered soil. Microbial Ecology 64: 79–90.

Lefèvre E, Bardot C, Noël C, Carrias JF, Viscogliosi E, Amblard C, Sime-Ngando T. 2007. Unveiling fungal zooflagellates as members of freshwater picoeukaryotes: evidence from a molecular diversity study in a deep meromictic lake. Environmental Microbiology 9: 61–71.

Lefèvre E, Roussel B, Amblard C, Sime-Ngando T. 2008. The molecular diversity of freshwater picoeukaryotes reveals high occurrence of putative parasitoids in the plankton. PLoS One 3: e2324.

Lepère C, Domaizon I, Debroas D. 2008. Unexpected importance of potential parasites in the composition of the freshwater small-eukaryote community. Applied and Environmental Microbiology 74: 2940–2949.

Letcher PM, Powell MJ. 2012. A taxonomic summary and revision of Rhizophydium (Rhizophydiales, Chytridiomycota). Alabama University Printing, No. 1. Imprint Tuscaloosa, USA.

Letcher PM, Powell MJ, Barr DJS, Churchill PF, Wakefield WS, Picard KT. 2008. Rhizophlyctidales – a new order in Chytridiomycota. Mycological Research 112: 1031–1048.

Letcher PM, Powell MJ, Chambers JG, Holznagel WE. 2004. Phylogenetic relationships among Rhizophydium isolates from North America and Australia. Mycologia 96: 1339–1351.

Letcher PM, Powell MJ, Churchill PF, Chambers JG. 2006. Ultrastructural and molecular phylogenetic delineation of a new order, the Rhizophydiales. Mycological Research 110: 898–915.

Longcore JE. 1995. Morphology and zoospore ultrastructure of Entophlyctis luteolus sp. nov. (Chytridiales): implications for chytrid taxonomy. Mycologia 87: 25–33.

Longcore JE. 1996. Chytridiomycete taxonomy since 1960. Mycotaxon 60: 149–174.

Longcore JE, Simmons DR. 2012. The Polychytriales ord. nov. contains chitinophilic members of the rhizophlyctoid alliance. Mycologia 104: 276–294.

Luo W, Kotut K, Krienitz L. 2013. Hidden diversity of eukaryotic plankton in the soda lake Nakuru, Kenya, during a phase of low salinity revealed by a SSU rRNA gene clone library. Hydrobiologia 702: 95–103.

Mamkaeva MA, Pljusch AV, Mamkaeva KA. 2006. Some peculiarities of Rhizophydium mammillatum strains isolated from fresh-water reservoirs of North-West region of Russia. Mycologia i Phytopathologia 40: 402–410. In Russian.

Medlin L, Elwood HJ, Stickel S, Sogin ML. 1988. The characterization of enzymatically amplified eukaryotic 16S-like rRNA-coding regions. Gene 71: 491–499.

Mohamed DJ, Martiny JB. 2011. Patterns of fungal diversity and composition along a salinity gradient. ISME Journal 5: 379–388.

Monchy S, Sanciu G, Jobard M, Rasconi S, Gerphagnon M, et al. 2011. Exploring and quantifying fungal diversity in freshwater lake ecosystems using rDNA cloning/sequencing and SSU tag pyrosequencing. Environmental Microbiology 13: 1433–1453.

Mozley-Standridge SE, Letcher PM, Longcore JE, Porter D, Simmons DR. 2009. Cladochytriales – a new order in Chytridiomycota. Mycological Research 113: 498–507.

Naff CS, Darcy JL, Schmidt SK. 2013. Phylogeny and biogeography of an uncultured clade of snow chytrids. Environmental Microbiology 15: 2672–2680.

Powell MJ. 1978. Phylogenetic implications of the microbody-lipid globule complex in zoosporic fungi. Biosystems 10: 167–180.

Rabenhorst L. 1864–1868. Flora Europaea Algarum Aquae dulcis et Submarinae. Vol. 3. Kummer, Leipzig, Germany.

Ronquist F, Huelsenbeck JP. 2003. MrBayes 3: Bayesian phylogenetic inference under mixed models. Bioinformatics 19: 1572–1574.

Simmons DR. 2009. Cladochytriales – a new order in the Chytridiomycota. Mycological Research 113: 498–507.

Simmons DR, James TY, Meyer AF, Longcore JE. 2009. Lobulomycetales, a new order in the Chytridiomycota. Mycological Research 113: 450–460.

Sparrow FK. 1960. Aquatic Phycomycetes, 2nd edn. University of Michigan Press, Ann Arbor, USA.

Sridhar KR, Beaton M, Bärlocher F. 2011. Fungal propagules and DNA in feces of two detritus-feeding amphipods. Microbial Ecology 61: 31–40.

Stamatakis A. 2006. RAxML-VI-HPC: maximum likelihood-based phylogenetic analyses with thousands of taxa and mixed models. Bioinformatics 22: 2688–2690.

Thomas MC, Selinger LB, Inglis GD. 2012. Seasonal diversity of planktonic protists in Southwestern Alberta rivers over a 1-year period as revealed by terminal restriction fragment length polymorphism and 18S rRNA gene library analyses. Applied and Environmental Microbiology 78: 5653–5660.

Zhang X, Ma X, Wang N, Yao T. 2009. New subgroup of Bacteroidetes and diverse microorganisms in Tibetan plateau glacial ice provide a biological record of environmental conditions. FEMS Microbiology Ecology 67: 21–29.